An assumption for laser zone refining applied in the lunar

Liping Wang, Guangshi Li*, Lang Che, Hongwei Cheng, Xingli Zou, Qian Xu, Xionggang Lu
School of Materials Science and Engineering & State Key Laboratory of Advanced Special Steels, Shanghai University
Shanghai, P.R.C
*co-corresponding authors: G.S. Li, lgs@shu.edu.cn

***Abstract*—With the development of lunar exploration, researches have proposed a large number of techniques for In-Situ Resource Utilization (ISRU). Due to microgravity in the Moon, traditional metallurgy such as cold hearth melting is hard to refining metals or alloys. Hence, this paper proposed a new zone refining technique using solar-pump laser as heat source, which would be a potential titanium metallurgical technique in the lunar in future. Numerical simulation and thermodynamic equilibrium distribution calculation were conducted in order to investigate the theoretical feasibility of titanium zone refining using laser heating. The results show that laser zone refining is capable of segregation of titanium and iron in theory. Thus, the design of zone refining of titanium in lunar implementing appropriate laser parameters is possible to be successful in the near future.**

Keywords—laser heating, zone refining, titanium

I. INTRODUCTION

From the Chinese ancient mythology “Chang’e flying to the moon” to the American astronaut’s landing on the moon for the first time, human’s imagination and exploration to lunar have never stopped. Nowadays, building a permanent lunar base, developing and utilizing the moon’s resources, taking the moon as a transit station and walking to the deep space [1] have become international lunar exploration’s final goals. It is obviously impossible to bring everything needed to the lunar construction and human activities from the earth. Hence, In-Situ Resource Utilization (ISRU)[2], a kind of technology that harnesses the Moon’s or the Mars’s air, water ice, soil, mine and other resources to create human long-term survival demand including oxygen, water, food, propulsion and so on, represents a critical concept in human lunar exploration and deep space exploration.

It is estimated that there are 1300-1900 trillion tons of ilmenite ($FeTiO_3$) in the lunar basalts. Hence, people can directly gain abundant oxygen, iron and titanium through reduction of ilmenite by hydrogen on the Moon, which is a kind of ISRU, attracting great interest [3]. However, if reduced titanium is expected to utilize further such as fabricating, modifying aerospace products and manufacturing building materials, it needs to be refined because there must be impurity elements in it like Fe, Al, Mg and other elements made up of lunar soil. Cold hearth melting (CHM) [4]is the most common method to refine titanium and titanium alloy in the Earth, which is divided into electron beam cold hearth melting (EBCHM) and plasma arc cold hearth melting (PACHM) in terms of different heat sources. One of the main refining principles of CHM is to deposit high-density inclusions and to float of low-density inclusions. Unfortunately, due to the low gravity environment on the Moon (only 1/6 of the Earth’s), the above mentioned factor become ineffective so we have to find another refining method as ISRU to eliminate impurities in Ti on the Moon.

Zone melting (ZM)technique, invented by American scientist W. G. Pfann in 1952[5], is one of the most promising methods for preparation of high-purity metal. There are three factors of eliminating impurities by ZM as follow [6,7]: (1) separating impurities with different distribution coefficients into different positions of metal rod; (2) evaporating lower vapor pressure of metals in high vacuum; (3) degassing non-metallic elements from metal matrix like H, N, O, etc. There are no effects of buoyancy convection, sedimentation and hydrostatic pressure caused by gravity on metallurgical process under microgravity condition of the Moon while surface tension and diffusion become the main controlling factors. Therefore, a new thought was proposed here that ZM taking solar-pumped laser [8] as heat source will be developed to refine and produce high purity Ti and Ti alloy in suit.

This paper aimed at demonstrating the theoretical feasibility of the thought because there were few articles about laser zone melting and no such experiment conducted on the Moon. In the present paper, we have established a 2D transient model comprising the basic conservation principles, the governing equations and the considered physical effects to investigate the process of laser zone refining Ti alloy. The model shows the temperature distribution, and the formation of the molten pool (including the dimension, the travel rate and the fluid dynamics). In addition, the effect of gravity on the process was studied. After that, the results of the simulation were used to calculate the effective distribution coefficient and the distribution profile of impurity element Fe in Ti.

II. NUMERICAL SIMULATION

It is necessary to numerically simulate laser zone refining process to help us know the physical phenomenon and to provide process optimization because few articles on this have been reported by now. Moreover, numerical simulation is a highly efficient and cost-saving kind of pre-experimental method.

A detailed description of physical phenomenon of laser zone refining Ti alloy needs to be introduced first before simulation.

A. Physical Phenomenon

A Ti alloy rod as a sample was set in a copper crucible under a vacuum environment. When the laser beam moving laterally radiated the Ti rod, energy was absorbed at the surface of the rod at a certain absorption coefficient. Heat conduction happened inside the material and between the Ti rod and the copper crucible. The rod started to melt at the melting point meanwhile it absorbed the latent heat. The Marangoni effect (and the gravitational force) led to fluid flow in the melt pool. The heat loss was caused by radiation. The melt pool solidified and the later position of the rod melted with the movement of the laser until the process ended.

Fig. 1 shows schematic representation of the laser zone refining. Table I and II respectively give process parameters and material data.

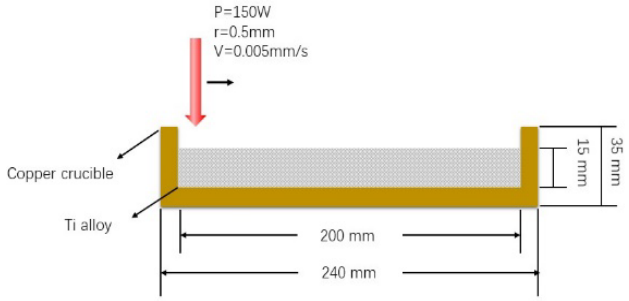

Fig. 1. Schematic representation of the laser zone refining.

TABLE I. PROCESS PARAMETERS

Process parameter	Unit	Value
Laser power	W	150
Beam radius	mm	0.5
Feed velocity	mm/s	0.005

TABLE II. MATERIAL DATA

material	material properties	Unit	Value
Ti alloy	density [9]	kg/m^3	1173(solid) 1940(liquid)
	heat capacity [10]	J/(kg.K)	520
	thermal conductivity [10]	W/(m.K)	21.9
	dynamic viscosity [11]	Pa.s	0.0032
	surface tension coefficient [11]	N/m.K	-2.4×10^{-4}
	absorption coefficient [12]	-	0.4
	melting temperature [13]	K	1928.2
	latent heat of melting [9]	kJ/kg	391
	emissivity	-	0.3
Copper [14]	density	kg/m^3	8960
	heat capacity	J/(kg.K)	385
	thermal conductivity	W/(m.K)	377

B. Mathematical Model

1) Governing equations

Equations of conservation of mass, momentum and thermal energy are formulated in (1) ~ (3).

Continuity equation:

$$\frac{\partial \rho}{\partial t} + \nabla \rho \vec{u} = 0 \quad (1)$$

where ρ is the density and u is the velocity vector of fluid flow in molten pool.

The heat conduction equation:

$$\rho C_p \frac{\partial T}{\partial t} + \rho C_p u.\nabla T = \nabla(k\nabla T) + Q_{laser} \quad (2)$$

where ρ is the density, C_p represents the specific heat capacity, u is the velocity vector, k is the thermal conductivity, and Q_{laser} is the source term.

The fluid dynamics of the model is based on incompressible Navier-Stokes equation:

$$\rho \frac{\partial u}{\partial t} + \rho(u.\nabla)u = -\nabla p + \mu \nabla^2 u + \rho g + F_g + F_{mar} \quad (3)$$

with the velocity u, the pressure p, the dynamic viscosity μ, the gravity constant g, the volume force F_σ and the Marangoni force F_{mar}. In this model, the solid is assumed as fluid, which dynamics viscosity is 1000 Pa.s [15].

Non-isothermal flow couples the temperature filed and the flow field, as in (4):

$$-n.q = \rho C_p C_\mu^{\frac{1}{4}} k^{\frac{1}{2}} \frac{T_w - T}{T_{amb}} \quad (4)$$

where n is the normal direction to the wall, q is the heat flux, ρ is the density, C_p is the special heat capacity, k is the thermal conductivity, T_w denotes the reference temperature of the wall equals to 297.15K.

The phase change of melting is considered into the model by using equivalent enthalpy method.

$$C_p = C_p^*(T) + \frac{1}{\Delta T.\sqrt{\pi}} e^{(\frac{T-T_m}{\Delta T})}.L_m \quad (5)$$

$C_p^*(T)$ represents the heat capacity depending on temperature, ΔT represents temperature range of 10 K, T_m is melting point of material and L_m is melting latent heat.

2) Initial and boundary conditions

Initial conditions: At the beginning of the refining process, the initial temperature of the sample is equal to the ambient room temperature T_{amb}=T| t=0=293.15K.

Laser flux, thermal radiation and Marangoni effective are applied on the top surface. The source term is simulated as a surface heat source with Gaussian distribution, as in (6):

$$Q_{laser} = \frac{AP}{2\pi r^2} e^{\frac{-[(x-vt)^2+y^2]}{2r^2}} \quad (6)$$

with A the absorption coefficient, P the laser power, r the laser beam radius, v the feed velocity.

Thermal radiation is calculated by Stefan-Boltzmann law, as in (7):

$$-k\frac{\partial T}{\partial y}=\sigma\varepsilon(T^4-T_{amb}^4) \quad (7)$$

where σ is the Stefan-Boltzmann constant, ε is emissivity of Ti alloy.

Due to variations of the surface tension coefficient with temperature, Marangoni effect causes the fluid flow in the molten pool, as in (8)

$$[-pI+\mu(\nabla u+(\nabla u)^T)-\frac{2}{3}\mu(\nabla.u)I]n=\gamma\nabla T \quad (8)$$

where p is the pressure, I is the identity matrix, μ is the dynamic viscosity, ∇u is the gradient of the velocity, γ is the surface tension depending on temperature and ∇T is the gradient of the temperature.

Buoyancy force is applied in the Boussinesq approximation to take into the volumetric change account due to thermal expansion.

$$F_g=\rho g\beta_T(T-T_m) \quad (9)$$

where F_g denotes buoyancy force, ρ is density, g is the gravity constant, β_T is thermal expansion and T_m is melting temperature.

The other boundaries exposed to the environment are assumed as thermal insulting boundaries:

$$-k\frac{\partial T}{\partial n}=0 \quad (10)$$

with k the conductivity coefficient and n the normal direction of the boundary.

C. Geometry and Mesh

The geometric dimensions of the Ti alloy sample and the copper crucible are shown in Fig.1.

On the top surface, the mesh is refined where the laser beam passes during the whole computation. For the cooper crucible, maximum element size of 8.88mm and minimum element size of 0.03cm are defined respectively. In the finite element model, there are 6471 triangular units, 16000 quadrilateral units and 19490 mesh vertices.

III. Calculation Of Distribution Condition

The ZM technique consists of producing a liquid zone in a heated sample rod and slowly moving it along the rod, causing impurity element to become redistributed inside the sample due to its different solubility in solid and liquid, namely distribution coefficient. Consequently, it is essential to know impurity element's distribution coefficient and to further understand the mechanism responsible for the impurity redistribution during the process.

The equilibrium distribution coefficient k_0 is acquired from the binary phase diagram of matrix and impurity metal when the solidification is processed slowly. The impurity whose k_0 is over 1 moves to the starting position, conversely, the one whose k_0 is below 1 gathers in the end of the rod after segregation. If k_0 be equal to 1, which means no segregation of the impurity between solid and liquid, the refine efficient is poor.

In fact, solidification is generally normal freezing where effective distribution coefficient k_{eff} is in charge. k_0 and k_{eff} can be defined by the following equation [16].

$$k_{eff}=(\frac{k_0}{k_0+(1-k_0)\exp(-f\delta/D)}) \quad (11)$$

where f, δ, D are the S/L interface travel rate, the thickness of diffusion boundary and the diffusion coefficient. If diffusion is an only mixing process, δ is of the order of the zone length. If convection currents exists, δ is approximately 1 mm, and can be reduced to 0.1 mm by moderate stirring and to 0.01 mm by vigorous stirring [16].

After one pass of a molten zone, the composition distribution taking the degree of mixing in the liquid into account is given in (12) and (13) [16].

When $0\leqslant X<1-Z$, the impurity concentration in solid can be calculated as follow:

$$C_s=C_0[1-(1-k)\exp(-\frac{kX}{Z})] \quad (12)$$

When 1-Z⩽X⩽1, it follows that

$$C_s=C_0\{1-(1-k)\exp[-\frac{k(1-Z)}{Z}]\}\times\{1-[\frac{X-(1-Z)}{Z}]\}^{k-1} \quad (13)$$

where $Z=\frac{z}{L}$ and $X=\frac{x}{L}$ are dimensionless variables. L is the length of the sample rod, z is the length of the molten zone and x is the distance from the beginning of the sample rod, as shown in Fig. 2.

In this paper, we tried to calculate k_{eff} of impurity element Fe in Ti and the distribution curve after one pass of refining by using the results of f and z from the aforementioned numerical simulation. The results will be analyzed in detail in the section IV.

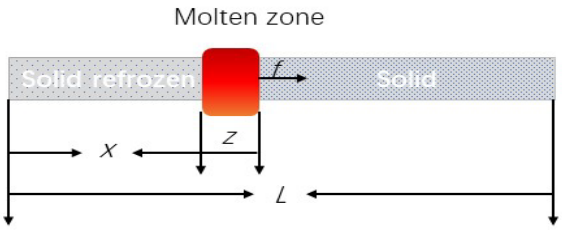

Fig. 2. Schematic representation of a zone refining process.

IV. Results And Discussion

A. Temperature Evolution

Fig. 3 shows the temperature field of the sample rod and the copper crucible with time during laser radiation. There is large temperature gradient between the radiated area and the vicinity. The laser intensity is the highest at the center of laser beam in case of Gaussian heat source. Due to thermal radiation on the top surface and heat conduction with the copper crucible, the sample rod losses heat energy after laser leaves. In that case, heated material happens to melt and solidify. Fig.4 displays the maximum and the minimum

temperature of the sample rod versus time curves. It is indicated that there are rapid increase and decrease in the sample rod temperature at the beginning and end of the zone refining. The temperature fluctuations in the molten pool are small in the middle so the presence of the molten pool is stable. A stationary temperature gradient is a benefit to improve refining effect [17]. The temperature of the Ti alloy decreases below the melting point, indicating zone refining is finished.

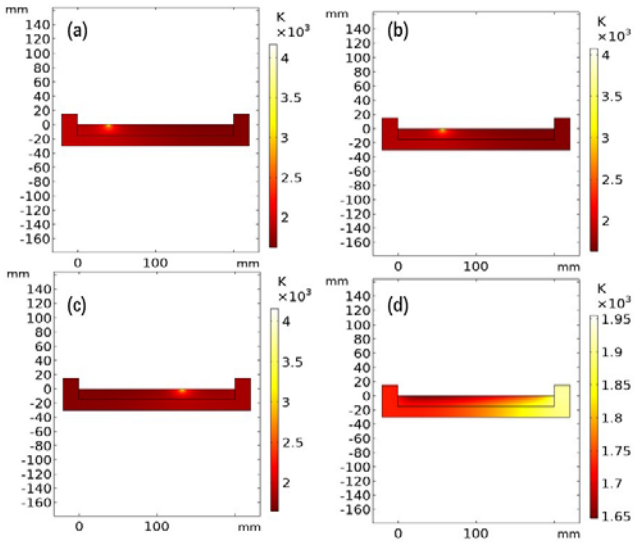

Fig. 3. The evolution of temperature field with time: (a) at 8000s (b) at 11450s (c) at 26500s (d) at 40150s.

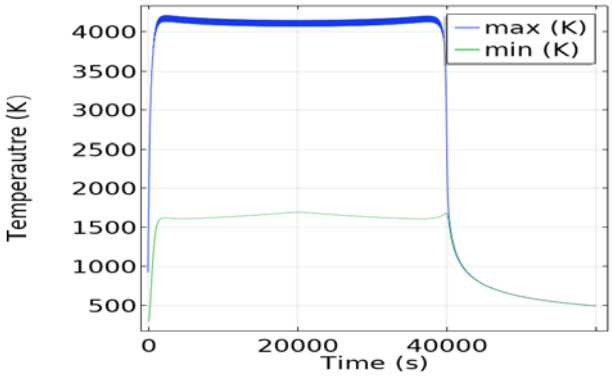

Fig. 4. The maximum and the minimum temperature of the sample rod versus time curves.

B. Volume Fractions of Liquid Phase and Marangoni Convection

The shape and the flow field of the molten zone can be acquired from Fig.5. Due to a Gaussian distribution for the laser heat source, the shape of the molten zone is like a cavity, having maximum depth at the center. The shape and the size of the molten zone remain approximately constant during this process, which also confirms the stability of the molten zone. The average length of the melting zone is equal to 31.9 mm. The result will be used to compute the distribution curve of Fe in Ti.

In addition, the black arrows displayed in Fig.5 offer insight into the flow direction of the melt. Because of a negative temperature-dependent coefficient of surface tension, flow is radially symmetric and goes from the center to the boundaries of the molten pool. The flow velocity near the top surface is higher than the one near the bottom mushy zone.

The fluid flow caused by Marangoni force is more primary than buoyancy force. Hence, the latter's effect is so little that there is no obvious difference in flow field between two models (the one considering buoyancy force and another not).

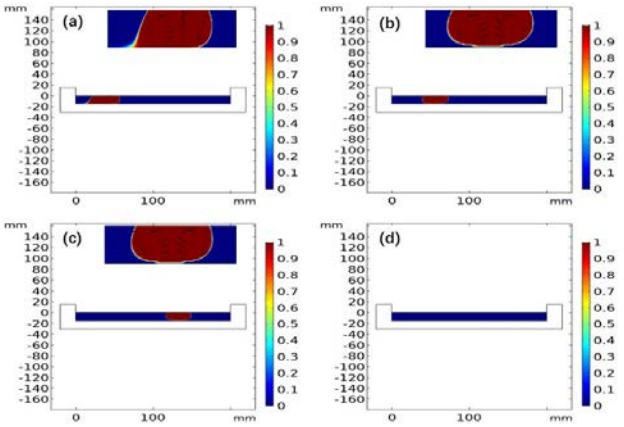

Fig.5. The evolution of fluid field with time: (a) at 8000s (b) at 11450s (c) at 26500s (d) at 40150s.

The conclusion made from Fig.5 (d) that all Ti alloy has solidified at 40150s is consistent with the above one. Moreover, the travel rate of the molten zone is calculated, whose value is 0.005 mm/s. More noteworthy is that Marangoni effect driving stirring in the molten pool is able to promote impurity transportation [18,19].

C. k_{eff} and the Distribution Curve of Fe in Ti

Firstly, we assumed that the initial concentrate of Fe in Ti is 0.25 mol/l. Then, k_0 and D were given the values used in other literatures, k_0=0.39[20] and D=10^{-5} cm^2/s[13]. δ is estimated to be 0.1mm due to the presence of stirring. According to (11), k_{eff} is equal to 0.51. At last, the Fe distribution curve after one refining pass is given in Fig.6. The tendency that the content of the impurity decreases obviously at the starting position, keeps steady at the middle and rapidly rises at the end is in good agreement with other literatures [5,21]. The concentration of Fe decreases by 48.8% at the beginning of the sample and rise highly at the end, which means cutting the tail can acquire the high purity Ti.

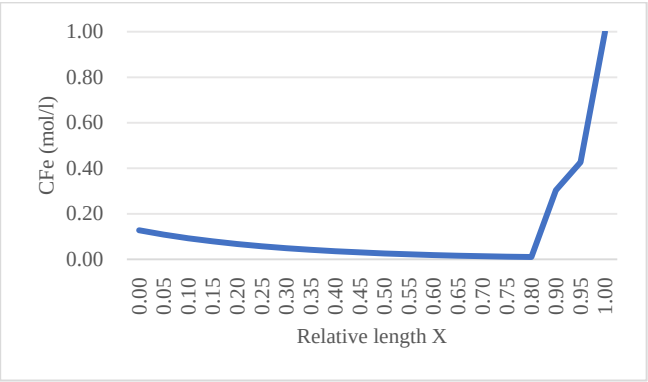

Fig.6. The diffusion profile of Fe in Ti after one zone pass.

V. Conclusions And Prospects

The current work presents investigations on the feasibility of laser zone refining by numerical simulation

and calculations of distribution coefficient and distribution profile. The simulation was performed in order to describe the process taking place, in particular, melting, flow fluid and freezing, i.e. Analyzing the simulation results, it is found that a stable molten zone can be formed when laser power is 150 W, laser beam radius is 0.5 mm and feed velocity is 0.005 mm/s. The convection in molten pool is primarily driven by Marangoni force so it is speculated that microgravity in the Moon have little influence on zone refining. After that, k_{eff} and the composition profile after a zone pass of Fe in Ti were calculated by combing the results of the numerical simulation. The 0.51 of k_{eff} means that Fe will transfer to liquid phase and is concentrated in the tail of Ti rod. The composition curve detailly shows the distribution of Fe in Ti after a zone pass. Consequently, laser zone refining is capable of segregation of Ti and Fe in theory and potentially becomes an ISRU technic applied in the Moon.

In order to further research how to apply laser zone refining as ISUR in the Moon, more work will be done focusing on the following points: (1) improving the model by considering degassing of non-metallic impurities and removal of volatile metallic ones; (2) establishing a more accurate model based on the actual moon environment; (3) analyzing impact of different impurities and calculating impurity distribution after several pass numbers. (4) operating experiments in order to verify the simulation and the calculation results in the future.

ACKNOWLEDGMENT

The funding for this work was provided by Steel Joint Research Foundation of National Natural Science Foundation of China–China Baowu Iron and Steel Group Co. Ltd. (Grant No. U1860203), the “Super Postdoctoral” Incentive Program in Shanghai, National Natural Science Foundation of China (Grant No. 51576164) and the CAS Interdisciplinary Innovation Team. The authors also wish to thank other colleagues (such as Dr. Chengteng Sun and Dr. Hui Liu et al) in Shanghai University for their active supports and constructive comments.

REFERENCES

[1] M. B. Duke, W. W. Mendell, and B. B. Roberts, “Strategies for a permanent lunar base,” Lunar Bases & Space Activities of Century, 1985.

[2] G. B. Sanders and W. E. Larson, “Progress Made in Lunar In Situ Resource Utilization under NASA's Exploration Technology and Development Program,” Earth and Space 2012, 2012, pp. 457-478.

[3] H. M. Sargeant, F. A. J Abernethy, and S. J. Barber, “Hydrogen reduction of ilmenite: Towards an in situ resource utilization demonstration on the surface of the Moon,” Planetary and Space Science, 2019, pp. 104751.

[4] M. J. Cen, Y. Liu, and X. Chen, “Inclusions in melting process of titanium and titanium alloys,” China Foundry, 2019.

[5] W. G. Pfann, “Principles of Zone-Melting,” JOM, vol. 4, pp. 747-753, 1952.

[6] G. M. Lalev, J. W. Lim, and N. R. Munirathnam, “Impurity behavior in Cu refined by Ar plasma-arc zone melting,” Metals & Materials International, vol. 15, pp, 753-757, 2009.

[7] G. M. Lalev, J. W. Lim, and N. R. Munirathnam, “Concentration Behavior of Non-Metallic Impurities in Cu Rods Refined by Argon and Hydrogen Plasma-Arc Zone Melting,” Materials Transactions, vol. 50, pp. 618, 2009.

[8] D. Guilhot, P. Ribes-Pleguezuelo, “Laser Technology in Photonic Applications for Space,” Instruments, vol. 3, pp.50, 2019.

[9] M. Wu, I. Wagner, and P. R. Sahm, “Casting of Ti prostheses and implants with the Aid of numerical simulation,” JOM, vol, 53, pp. 36-38, 2010.

[10] N, Ren, L. Jiang, and L. Dan, “Comparison of the simulation and experimental of hole characteristics during nanosecond-pulsed laser drilling of thin titanium sheets,” International Journal of Advanced Manufacturing Technology, vol. 76, pp. 735-743, 2015.

[11] D. Höche, S. Müller, and G. Rapin, “Marangoni Convection during Free Electron Laser Nitriding of Titanium,” Metallurgical and Materials Transactions B, vol 40, pp 497-507, 2009.

[12] J. Xie, A. Kar, and J. A. Rothenflue, “Temperature - dependent absorptivity and cutting capability of CO2, Nd:YAG and chemical oxygen–iodine lasers,” Journal of Laser Applications, vol. 9, pp. 77-85, 1997.

[13] G. B. Gibbs, D. Graham and D. H. Tomlin, “Diffusion in titanium and titanium—niobium alloys,” The Philosophical Magazine: A Journal of Theoretical Experimental and Applied Physics, vol. 8 pp 1269-1282, 1963.

[14] D. G. Gunjo, S. R. Jena, and P. Mahanta, “Melting enhancement of a latent heat storage with dispersed Cu, CuO and Al2O3 nanoparticles for solar thermal application,” Renewable Energy, vol. 121, pp. 652-665, 2018.

[15] V.Bruyere, C. Touvrey, and P.Namy, “A Phase Field Approach to Model Laser Power Control in Spot Laser Welding,” the 2014 COMSOL Conference in Cambridge, 2015.

[16] J.A.Spim Jr., M. J. S. Bernadou, A. Garcia “Numerical modeling and optimization of zone refining,” Journal of Alloys & Compounds, , vol. 298, pp. 299-305, 2000.

[17] W. G. Pfann, “Temperature Gradient Zone Melting,” JOM, vol. 7, p. 961-964, 1955.

[18] D. Hoeche, S. Müller, and G. Rapin, “Marangoni Convection during Free Electron Laser Nitriding of Titanium,” Metallurgical and Materials Transactions B, vol. 40, pp. 497-507, 2009.

[19] E. Louvis, P. Fox, and C. J. Sutcliffe, “Selective laser melting of aluminium components,” Journal of Materials Processing Technology, vol. 211, pp. 275-284, 2011.

[20] J. K. Kivilahti, O. B. Tarasova, “The determination of the Ti-rich liquidus and solidus of the Ti-Fe system,” Metallurgical Transactions A, vol. 18, pp. 1679-1680, 1987.

[21] M. Nakamura, M. Watanabe, and K. Tanaka, “Zone Refining of Aluminum and Its Simulation,” Materials Transactions, vol 55, pp. 664-670, 2014.